JOURNAL

OF THE AMERICAN CHEMICAL SOCIETY

VOLUME 110, NUMBER 21 OCTOBER 12, 1988

Linkage Position in Oligosaccharides by Fast Atom Bombardment Ionization, Collision-Activated Dissociation, Tandem Mass Spectrometry and Molecular Modeling. L-Fucosyl$_p$-(α1→X)-D-*N*-acetyl-D-glucosaminyl$_p$-(β1→3)-D-galactosyl$_p$-(β1-*O*-methyl) Where X = 3, 4, or 6[†]

Roger A. Laine,*,‡,§ Krishna M. Pamidimukkala,‡ Alfred D. French,∥ Randall W. Hall,§ Saeed A. Abbas,⊥ Rakesh K. Jain,⊥ and Khushi L. Matta⊥

Contribution from the Departments of Biochemistry and Chemistry, Louisiana State University and A & M College, and The LSU Agricultural Center, Baton Rouge, Louisiana 70803, Southern Regional Research Center, USDA, P.O. Box 19687, New Orleans, Louisiana 70179, and Department of Gynecological Oncology, Roswell Park Memorial Institute, Buffalo, New York 14263. *Received March 9, 1988*

Abstract: Fast atom bombardment mass spectra (FABMS), and collision-activated dissociation (CAD) studies of three synthetic, linkage-isomeric trisaccharides were conducted to assess whether ion patterns could distinguish among the three possible different linkage positions of the terminal fucose in the following otherwise identical structures:

L-fucosyl$_p$-(α1→3)-D-*N*-acetylglucosaminyl$_p$-(β1→3)-galactosyl$_p$-(β1-*O*-methyl) (F3)

L-fucosyl$_p$-(α1→4)-D-*N*-acetylglucosaminyl$_p$-(β1→3)-galactosyl$_p$-(β1-*O*-methyl) (F4)

L-fucosyl$_p$-(α1→6)-D-*N*-acetylglucosaminyl$_p$-(β1→3)-galactosyl$_p$-(β1-*O*-methyl) (F6)

FABMS, low-energy CAD spectra were recorded for the protonated molecular ions as well as for major fragment ions occurring in the FABMS spectra. The rationale was that differences in internal, nonbonding free energy and entropic terms such as degrees of freedom of motion near minimum energy conformations could allow threshold CAD experiments to distinguish among the three structures, resulting in a statistically higher percentage of bond cleavage for more sterically hindered bonds. Structures with more freedom of motion would more readily dissipate energy absorbed from collision events due to lowered probability of populating the reaction coordinate for glycosidic bond cleavage. Repeatability was ensured by choosing a standard survival percentage for the collided ion in one compound and comparing CAD spectra for the remaining compounds at the same instrument settings. CHEM-X and MMP2 (version 1985) molecular modeling programs were used to calculate minimum energy structures for the fucosyl→GlcNAc moieties and freedom of motion volumes near these minima among the three trisaccharides. Volumes of conformational freedom within 50 kcal above the minimum corresponded to density of states near the transition-state energy for bond cleavage. Observed CAD stability levels of molecular ions and observed intensity differences in product ions resulting from collision-activated glycosidic cleavages of fucosyl–GlcNAc bonds gave strong indications that steric factors in the positions of fucose linkage to GlcNAc in the three trisaccharides contribute to bond stability during CAD experiments in the relationship 6 > 4 > 3. This approach may provide another line of evidence for assignment of linkage positions in microgram quantities of intact saccharides where suitable standards are available.

Chemical determination of glycosidic bonds between saccharides is complex due to the many possible permutations of positions of sugar sequence, linkage, and anomeric configuration. The simplest formula for the number of possible structures S^* for an oligosaccharide comprised of a number N of different hexoses not repeated is $S^* = N! \times 2^{N_a} \times (4)^{N-1} \times 2^{N_r}$ for linear structures of one enantiomer. $N!$ is sugar epimer order, 2^{N_a} is anomeric configuration; position of linkage is $(4)^{N-1}$, and ring size (five- or six-membered) is 2^{N_r}, where N is the number of different hexoses in a chain comprised of single elements of each hexose.

For a linear string of five hexoses, the above calculation gives $S^* = 31\,457\,280$ chemically different structures. Allowing branching, repeated sugars, and D and L enantiomers greatly enlarges this number, producing $\sim 2 \times 10^9$ structures. These structures all have the same mass and share many physical properties. The numerically largest term $[(4)^{N-1}]$, is from position of linkage, which is also chemically the most difficult to determine.

* To whom correspondence should be addressed.

† This work was supported, in part, by NIH Grants 1RO1-GM35755, 1RO1DK24594, and DRR 02803 to R.A.L. and approved for publication by the Director of the Louisiana Agricultural Experiment Station as manuscript no. 88-12-2286.

‡ Department of Biochemistry, Louisiana State University and the LSU Agricultural Center.

§ Department of Chemistry, Louisiana State University.

∥ Southern Regional Research Center, USDA.

⊥ Roswell Park Memorial Institute.

0002-7863/88/1510-6931$01.50/0

Most biologically active carbohydrate epitopes, recognized by binding proteins, consist of six sugars or fewer,[1] thus, ultimately, most determinations of bioactive structures will involve saccharides of this size. As a model of specific binding proteins recognizing carbohydrate structures, the immune system in mammals is exquisitely sensitive to all of these parameters, antibodies recognizing as little as one change in an epimer, a position of linkage, or enantiomers. Obviously such a large store of possible information carried in a relatively small structure has not been ignored in evolution of biological systems. Increasing numbers of reports indicate that carbohydrates possess a great variety of important biological functions, including roles as anticlotting agents, immunomodulators, tumor antigens, growth factors, and genetic control elements, among others. Thus, it is important to find sensitive and rapid methods for structural determination.

Conventional Methodology for Linkage Determination. Position of linkage not only contributes the largest factor to the above calculation, it has also been the most difficult to attain structural parameter for small amounts of unknowns, due to the great number of chemical steps necessary for a complete analysis. The almost universally used method for linkage determination of samples >100 μg was developed by Lindberg's group in 1965–1970,[2-4] employing Hakomori's methylation procedure,[5] followed by release of the partially methylated sugars by hydrolysis. Sodium borohydride was used for reducing the resulting partially methylated aldoses to alditols and the product was acetylated. Combined gas chromatography–mass spectrometry was used to separate and identify the partially methylated alditol acetates.[2-4] An improvement in the sensitivity of this method was reported in 1981, using chemical ionization mass spectrometry,[6] allowing analysis down to 5–10 μg. Several improvements in the methylation reaction have also been reported, the most recent by Ciucanu and Kerek.[7] Other recent improvements are reviewed in the latter article. However, drawbacks to the method are the laborious 2-day chemical preparations required for each sample and chemical noise generated by the many steps of preparation.

Previous Work on Linkage Position Assignment by Mass Spectrometry of Oligosaccharides. Several approaches have been attempted to utilize mass spectrometry of oligosaccharides to assign position of linkage. Since the differences among the members of a set of oligosaccharides, all having the same molecular weight, may be limited to positional isomers and stereoisomers, mass spectrometric assignment of position of linkage within the intact molecules has not been extensively exploited. Several laboratories have assigned the *order* of monosaccharides of different mass within an oligomer, since fragmentation between saccharides requires cleavage of only one bond. Attempts to assign stereoisomers have been partially successful. Much of the relevant literature has been reviewed up through 1974 by Lonngren and Svensson.[8] Most of the attempts at direct mass spectral identification of linkage position have utilized various derivatives of carbohydrates or glycoconjugates and conventional EI mass spectrometry. One report showed discrimination among epimers of monosaccharides using chemical ionization (CI, isobutane) mass spectrometry,[9] and another showed differences in spectra of anomeric trimethylsilyl derivatives of monosaccharides.[10] Some linkages and anomeric configurations could be discerned in CI spectra of permethylated disaccharides by using various reagent gases.[11,12] Collision activation and chemical ionization (CI) in mass-analyzed ion kinetic energy spectra (MIKES) of permethylated disaccharides was used to discriminate among anomers in the complete set of glucose anomeric disaccharides.[13] While many or most of the same ions were present in each spectrum, collision activation allowed much more precise ratios among ions. These ratios were used for discrimination. Fast atom bombardment and MIKES technology were used for identification of aldohexoses[14,15] and anomeric methyl glycosides of otherwise underivatized glucose and galactose.[16] Stereoisomers of hexoses and 2-amino-2-deoxyhexoses were identified by tandem mass spectrometry and collision-activated dissociation (CAD).[17]

Kochetkov and his colleagues studied permethylated disaccharides having 1→2-, 1→4-, and 1→6-linked hexose residues.[18-20] This work led to a convention for the nomenclature of fragment ions from oligosaccharides.[21,22] Mass spectra were examined for 21 permethylated trisaccharides.[23] The monosaccharides and their sequences were assigned by primary and fragment ions from the first saccharide aA1, the second and third rings bcA1, the first and second rings baA1, and the reducing end ring cA1. The diagnostic value of other ions that might give position of linkage were noted in this study, but many of their origins and structures were unidentified.

In-Beam EIMS of Oligosaccharides. Indications of fragments relating to position of linkage have been reported in in-beam EI mass spectrometry of methylated and methylated and reduced glycosphingolipids.[24] Linkages attributed to types 1 and 2 A blood group determinants could be distinguished by m/z 182 in permethylated EI spectra of glycosphingolipids.[25,26] This work, in a group led by K. A. Karlsson, has made the most practical use of mass spectrometry data of intact compounds to give linkage positional information. Egge et al.[27] and Jardine et al.[28] also identified fragments in EI-MS of permethylated oligosaccharides which inferred some linkage positions.

FABMS Studies of Oligo- and Polylactosamine Series Oligosaccharides. Dell et al. successfully obtained molecular ion species and fragments in FABMS of lacto-*N*-tetraose as the peracetylated alditol.[29] Fukuda et al. confirmed the usefulness of this cleavage in FABMS studies of fragments of larger polylactosamines,[30] and

(1) Kabat, E. A. *J. Immunol.* **1960**, *84*, 82.
(2) Bjorndal, H.; Hellerqvist, C. G.; Lindberg, B.; Svensson, S. *Angew. Chem., Int. Ed. Engl.* **1970**, *9*, 610–619.
(3) Bjorndal, H.; Lindberg, B.; Svensson, S. *Carbohydr. Res.* **1967**, *5*, 433–440.
(4) Bjorndal, H.; Lindberg, B.; Pilotti, A.; Svensson, S. *Carbohydr. Res.* **1970**, *15*, 339–349.
(5) Hakomori, S.-I. *J. Biochem.* **1964**, *55*, 205–208.
(6) Laine, R. A. *Anal. Biochem.* **1981**, *116*, 383–390.
(7) Ciucanu, I.; Kerek, F. *Carbohydr. Res.* **1984**, *131*, 209–217.
(8) Lonngren, J.; Svensson, S. *Adv. Carbohydr. Chem. Biochem.* **1974**, *29*, 41–106.
(9) McNeil, M.; Albersheim, P. *Carbohydr. Res.* **1977**, *56*, 239.
(10) Murata, T.; Takahashi, S. *Carbohydr. Res.* **1978**, *62*, 1.
(11) de Jong, E. G.; Heerma, W.; Sicherer, C. A. X. G. F. *Biomed. Mass Spectrom.* **1979**, *6*, 242.
(12) de Jong, E. G.; Heerma, W.; Haverkamp, J.; Kamerling, J. P. *Biomed. Mass Spectrom.* **1979**, *6*, 72.
(13) de Jong, E. G.; Heerma, W.; Dijkstra, G. *Biomed. Mass Spectrom.* **1980**, *7*, 127–131.
(14) Puzo, G.; Prome, J. C. *Spectrosc. Int. J.* **1984**, *3*, 155–158.
(15) Puzo, G.; Fournie, J.-J.; Prome, J.-C. *Anal. Chem.* **1985**, *57*, 892–894.
(16) Puzo, G.; Prome, J.-C.; Fournie, J.-J. *Carbohydr. Res.* **1985**, *140*, 131–134.
(17) Wright, J. L. C.; Guevremont, R.; *Proceedings of the 35th ASMS Conference on Mass Spectrometry and Allied Topics*; 1987; pp 862–863.
(18) Chizhov, O. S.; Kochetkov, N. K. *Adv. Carbohydr. Chem.* **1966**, *21*, 29.
(19) Kochetkov, N. K.; Chizhov, O. S.; Bochkov, A. F. *MTP International Review of Science: Organic Chemistry Series One*; Butterworths, London, 1973; Vol. 7, p 147.
(20) Kochetkov, N. K.; Chizhov, O. S.; Poliakova, L. A. *Dokl. Akad. Nauk. SSSR* **1964**, *158*, 685.
(21) Kovacik, V.; Bauer, S.; Rosik, J.; Kovac, P. *Carbohydr. Res.* **1968**, *8*, 282.
(22) Kovacik, V.; Bauer, S.; Rosik, J.; Kovac, P. *Carbohydr. Res.* **1968**, *8*, 291.
(23) Karkkainen, J. *Carbohydr. Res.* **1971**, *17*, 1.
(24) Karlsson, K. A. *FEBS Lett.* **1973**, *32*, 317.
(25) Breimer, M. E.; Hansson, G. C.; Karlsson, K.-A.; Leffler, H.; Pimlott, W.; Samuelsson, B. E. *Biomed. Mass Spectrom.* **1980**, *6*, 231–241.
(26) Bjork, S.; Breimer, M. E.; Hansson, G. C.; Karlsson, K.-A.; Leffler, H. *J. Biol. Chem.* **1987**, *262*, 6758–6765.
(27) Egge, H.; Michalski, J. C.; Strecker, G. *Arch. Biochem. Biophys.* **1982**, *213*, 318–326.
(28) Jardine, I.; Matsuura, F.; Sweeley, C. C. *Biomed. Mass Spectrom.* **1984**, *11*, 562–568.
(29) Dell, A.; Morris, H. R.; Egge, H.; Von Nicolai, H.; Strecker, G. *Carbohydr. Res.* **1983**, *115*, 41–52.

Hanfland et al. applied the same technology to branched lactosamine fucoglycosphingolipids.[31] Indications of sugar order within the chain were apparent due to charge retention and glycosidic cleavages on the amino sugar, but there was no information in the spectra that gave indication of linkage position. Hounsell et al. investigated synthetic saccharides of the polylactosamine series with FABMS,[32] studied as the reduced oligosaccharides (alditols). Mass spectra of the tetrasaccharide *O*-methyl glycoside Gal-(β1→4)GlcNAc(β1→3)Gal(β1→4)GlcNAc(1→OMe) showed prominent ions with charge retention primarily on the amino sugar. Examples were ions at m/z 763 $[MH]^+$, 731 $[MH - 32]^+$, 366 [MH – reducing end disaccharide]$^+$. The $[GlcNAc]^+$ ion at m/z 204 was prominent in the lower mass range, but its presence or identity was not discussed by these authors. Negative ion FABMS studies by the latter group gave ions with charge retention on both neutral and amino sugar species, but linkage position was not indicated.

Other CAD Studies of Saccharide Structure. Positions of *O*-acetyl substituents on *O*-methyl xylopyranosides were reported to be assignable by using electron impact CAD mass spectra of the $[M - 32]^+$ ion.[33] Location of acetyl groups could not be unambiguously assigned in either EI- or CI-MS without CAD in the latter study. For the CAD spectra, the collision chamber was in the second field-free region of a reversed-geometry ZAB-2F VG instrument.[33] We have given a preliminary report[34] that significant information on position of linkage was present in FABMS–CAD spectra of synthetic heterotrisaccharides.

Rationale for Further CAD–MS Studies of Oligosaccharides

At a given collision energy, a series of oligosaccharides differing in one aspect of stereochemical structure, but otherwise identical, should show distinct, discriminating ion patterns if the formation of these ions depends on the chemical stability of the parent compound. Due to steric hindrance and differences in the number of degrees of freedom of motion (rotation and vibration) between sugars in various linkage positions within an oligosaccharide, chemical energy differences should be inherent in any pair or series of oligosaccharide isomers differing in one isomeric aspect. Linkage position and anomeric configuration may provide the largest factors to inequalities in chemical free energy, although epimer type also seems from the above-reviewed literature[13-17,33] to contribute measurable differences.

To perform a systematic study of the chemical information available for position of linkage in FABMS–CAD of saccharides, we have synthesized a series of isomeric trisaccharides differing only in the position of linkage of the terminal fucose. Computer models of the disaccharide portions that embody the differing linkages were constructed with CHEM-X software, and optimal conformations were sought through refinement with the program MMP2 (version 1985). These refined models were used with the CHEM-X van der Waals energy routines to construct energy surfaces for all possible rotations about the bonds to the oxygen atoms linking the disaccharides. The volumes of the energy wells approximate the freedom of motion available for each of the linkage types and, at the higher energies, indicate the range of states that are alternatives to the state corresponding to the reaction coordinate for glycosidic bond scission. approximate energy input to cleave the C1–O bond of a glycosidic linkage is estimated at 66 kcal, from an established value for C–O ether bonds.[35] We report here on low kinetic energy CAD studies and molecular energy calculations of three isomeric trisaccharides containing fucose, *N*-acetylglucosamine, and galactose as follows:

L-fucosyl$_p$-(α1→3)-D-*N*-acetylglucosaminyl$_p$-(β1→3)-D-galactosyl$_p$-(β1-*O*-methyl) (F3)

L-fucosyl$_p$-(α1→4)-D-*N*-acetylglucosaminyl$_p$-(β1→3)-D-galactosyl$_p$-(β1-*O*-methyl) (F4)

L-fucosyl$_p$-(α1→6)-D-*N*-acetylglucosaminyl$_p$-(β1→3)-D-galactosyl$_p$-(β1-*O*-methyl) (F6)

Experimental Section

Oligosaccharides were synthesized as described previously[36] and characterized by ^{13}C NMR. Fast atom bombardment (FAB) spectra were obtained on a Kratos MS80RFA or on a Finnigan TSQ70 using xenon and an Ion Tech Saddle-Field FAB gun at 8–9 keV. Collision-activated dissociation (CAD) studies were performed on the Finnigan TSQ70 with −10 to −100 eV of collision energy and 0.8 milliTorr of argon as collision gas. For CAD measurements, four to eight spectra from m/z 50 to 700 were averaged taken as 5-s scans. For Figure 1, spectra were recorded on a Kratos MS80RFA instrument using an Ion-Tech saddle-field atom gun and xenon as reagent gas, accelerated at 8.5 keV. Each intact oligosaccharide (10 μg) was dissolved in 1 μL of glycerol on a copper probe tip, and spectra were scanned at 30 s/decade from m/z 80 to 1200. For Figure 2 (Finnigan TSQ70), the experiment was set up at 0.8 millitorr of argon as collision gas and 25 eV of collision energy. Ions were generated by fast atom bombardment with xenon atoms at 8.5 keV. F3 (10 μg) was dissolved in 1 μL of glycerol. Five scans each were taken from m/z 50 to 600, first plotting CAD of m/z 544, then m/z 398, then m/z 350, and then m/z 204 (not shown). All five scans were averaged for representative spectra in succeeding figures. Experiments were repeated over 6 months to observe any changes from instrumental conditions. Molecular calculations were performed on a Digital Equipment Co. (DEC) MicroVax II using CHEM-X (Chemical Design Ltd, Oxford, England) and MMP2. The potential energy terms used in CHEM-X are as published by Giglio et al. (*Acta Crystallogr., Sect. B: Struct. Crystallogr. Cryst. Chem.* **1977**, *B33*, 2389) and include simple electrostatic monopole–monopole interactions using Coulomb's law as taken from the Giglio reference. A Heathkit 241 microcomputer (IBM-AT compatible) was used as a terminal to the MicroVax with the program EMU-TEK (FTG Data Systems) providing Tektronix 4105 emulation for the CHEM-X software. The 241 also ran the Hewlett-Packard 7475A pen plotter for energy contour maps which were made with TOPO and SURF from the SURFER package for IBM-PC and compatibles (Golden Software, Inc., Golden, CO).

Results and Discussion

In the FABMS spectrum of F3 [L-fucosyl$_p$-(α1→3)-D-*N*-acetylglucosaminyl$_p$-(β1→3)-D-galactosyl$_p$-(β1-*O*-methyl); Figure 1] the $[MH]^+$ ion occurred at m/z 544. In addition, significant fragmentation is apparent corresponding to losses of reducing end galactose methyl glycoside with cleavage of the GlcNAc C_1–O glycosidic bond accompanied by a hydrogen transfer from the GlcNAc to the galactose giving a nonreducing disaccharide ion at m/z 350. A loss of the fucose moiety from m/z 544 by cleavage of the fucose C_1–O glycosidic bond with a hydrogen transfer to GlcNAc (MH − 146) results in an ion at m/z 398, and loss of both neutral sugars in a like manner with charge retention on the *N*-acetylglucosamine results in a major fragment at m/z 204. Thus, the cleavage is characterized by scission of the C_1–O bond in each case, with transfer of H from the nonreducing side sugar to produce the ion. With charge retention on the amino sugar, either the reducing end galactose or nonreducing end fucose is lost, or both. Thus, ordering the sugars in the chain directly from the spectra is not trivial, but requires other knowledge of the structure. In this case, with the knowledge that the reducing terminal was an *O*-methyl glycoside, order could be inferred.

Since fragment ions of m/z 544 were apparent in the FABMS, fragment CAD experiments were possible. The FABMS spectra of all three compounds gave an ion representing $[2M + H]^+$ at m/z 1087 and ion adducts of $[M + glycerol]^+$ at m/z 635 and

(30) Fukuda, M.; Dell, A.; Fukuda, M. N. *J. Biol. Chem.* **1984**, *259*, 4782–4791.
(31) Hanfland, P.; Kordowicz, M.; Niermann, H.; Egge, H.; Dabrowski, U.; Peter-Katalinic, J.; Dabrowski, J. *Eur. J. Biochem.* **1984**, *145*, 531–542.
(32) Hounsell, E. F.; Madigan, M. J.; Lawson, A. M. *Biochem. J.* **1984**, *219*, 947–952.
(33) Kovacik, V.; Petrakova, E.; Mihalov, V.; Gvaroska, I.; Heerma, W. *Biomed. Mass Spectrom.* **1985**, *12*, 49–58.
(34) Pamidi, K. M.; Jain, R. K.; Abbas, S. A.; Matta, K. L.; Laine, R. A. *Proceedings of the 35th ASMS Conference on Mass Spectrometry and Allied Topics*; McKwen, C. N., Ed.; American Society for Mass Spectrometry: East Lansing, MI, 1987; pp 858–859.
(35) *Handbook of Chemistry and Physics, 64th ed.*; CRC: Boca Raton, FL, 1984; pp F187–F190.
(36) Jain, R. K.; Kohata, K.; Abbas, S. A.; Matta, K. L. *Carbohydr. Res.* **1988**, *172*, 27–35.

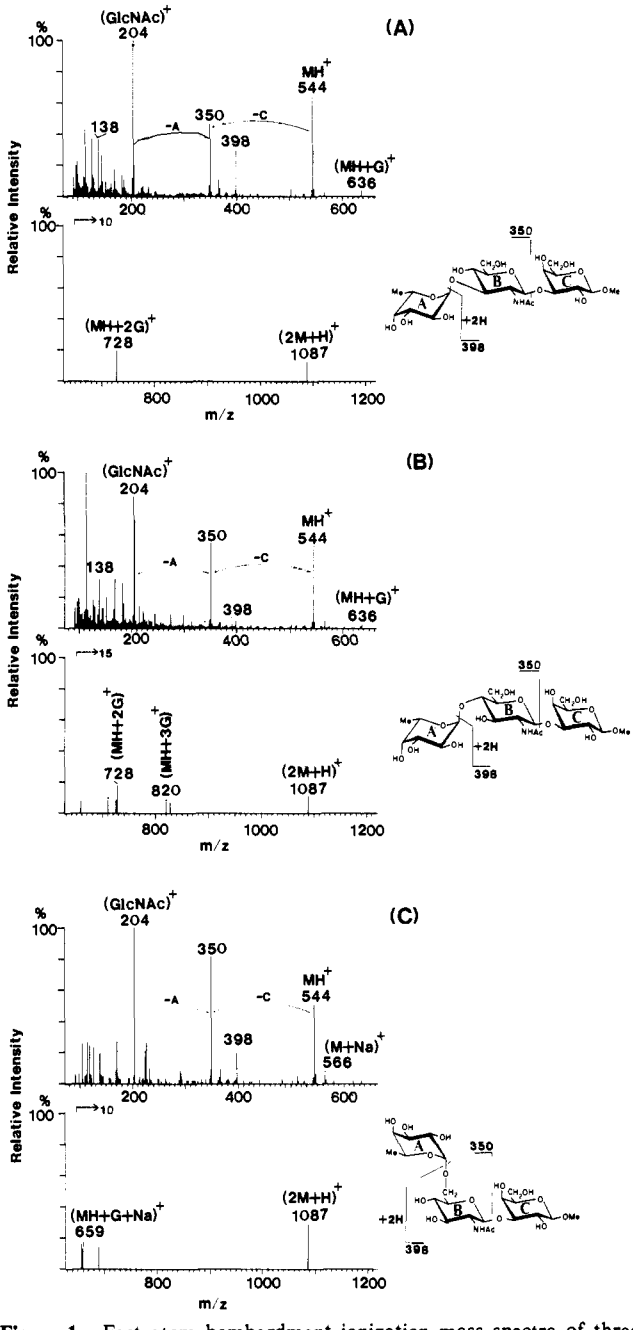

Figure 1. Fast atom bombardment ionization mass spectra of three trisaccharides designated F3, F4, and F6 (see text).

[M + 2glycerol]$^+$ at m/z 727, but no fragments were apparent from the m/z 1087 dimer. With no apparent fragments from ions larger than [MH]$^+$, the larger ions are useful for confirmation of the molecular weight of the oligosaccharide.

Products of m/z 544, 398, 350, and 204 in FABMS–CAD experiments were examined for differences relating to position of the fucose linkage to GlcNAc. Setting the survival rate of m/z 544 at 25% for F4, measurements for all other fragment ions were made at the same instrument settings. In practice, the most difficult parameter to measure was collision gas pressure. However, using incremented collision energy settings, we could reproduce the CAD cross section and survival rates regardless of small differences in collision gas pressure. For similar settings on the collision cell pressure gauge in several different experiments, a range of 25–40 eV gave similar survival of 25% of m/z 544 for F4. Figure 2 shows a typical experiment, recording five scans each of products of m/z 544, 350, and 204. Repeatability is apparent within each set.

Figure 3 compares products of m/z 544 for all three fucose linkages to GlcNAc. Setting the survival of F4 to 25%, F6 gave

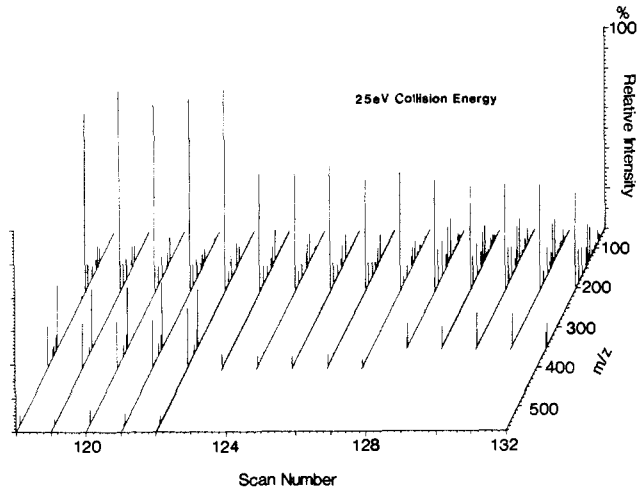

Figure 2. CAD experiment with F3 on Finnigan TSQ70: the experiment was set up at 0.8 millitorr of argon as collision gas and 25 eV of collision energy. Ions were generated by fast atom bombardment with xenon atoms at 8.5 keV. F3 (10 μg) was dissolved in 1 μL of glycerol. Five scans each were taken from m/z 50 to 600, first plotting CAD of m/z 544, then m/z 398, then m/z 350, and then m/z 204 (not shown). All five scans were averaged for representative spectra in succeeding figures.

a slightly higher survival at 28%. In contrast, at the same instrument settings, F3 had a much lower survival rate of m/z 544, close to 6%. Thus, the compound containing the 3-linkage seemed more labile. This was confirmed by observation in Figure 3 that production of the ion at m/z 398 (cleavage of the C_1–O bond of the terminal fucose linkage) is 4–5 times more facile for the 3-linkage F3 than for F4 or F6. The m/z 398 ion is less than 4% relative intensity for F4 (panel B) and F6 (panel C) and nearly 5 times as intense in F3 (panel A). In contrast, m/z 350 (loss of the reducing end galactose) appeared highest for F6, suggesting that the 6-linkage was more stable. The ratio m/z 350/398 was a strong indicator of linkage position in these spectra, in the order F6 > F4 > F3.

Another approach to the data in Figure 3 was to add the ion current for m/z 544 and 350, the combination of which contains the linkage in question, and compare the combined survival intensity to total ion current. The values measured were 15.9% survival for F3, 35.3% survival for F4, and 43.3% survival for F6 for a stability trend in the order F6 > F4 > F3.

To confirm stability of m/z 350 in F6, a comparison among F3, F4, and F6 for products of 350 is shown in Figure 4. While m/z 350 survival for F4 is 25% and 27% for F3 as shown in panels B and A, m/z 350 survived at 55% for F6, indicating far greater stability. Comparing the ratio of ion current for m/z 350 with total ion current in these spectra, F3 gave 7.8% survival, F4 gave 8.6%, and F6 remained at 12.8% to confirm the stability order F6 > F4 > F3. Distinct patterns for each linkage position were evident in ions lower than 204 as products of m/z 350. These patterns were consistent, and their fingerprints indicated fucose–>GlcNAc linkage position. The ions of lower mass than m/z 204 are products of 204 as shown in Figure 5. However, upon CAD of m/z 204, the ratio pattern of the products of 204 for all three compounds is nearly identical (Figure 5). This phenomenon may be due to the fact that m/z 204 as a product of m/z 350 has a different origin for each of the three linkages and therefore gives distinct product of m/z 350 patterns, but upon collision activation of m/z 204, any differences are scrambled, resulting in identical CAD patterns. The ratios of fragments of 204 within the CAD of m/z 350 are consistent patterns for each linkage type in this series. The proposed origin of these ions is as follows: m/z 186, (204 – water), m/z 168, (186 – water), m/z 138, (168 – HCHO), m/z 126, (186 – HOAc).

As shown in Figure 6, m/z 398 survived at 9% for F3, 12% for F4, and 20% for F6. This showed stability in the order F6 > F4 > F3. The product ion patterns look nearly identical, which would be expected since m/z 398 should be the same disaccharide in

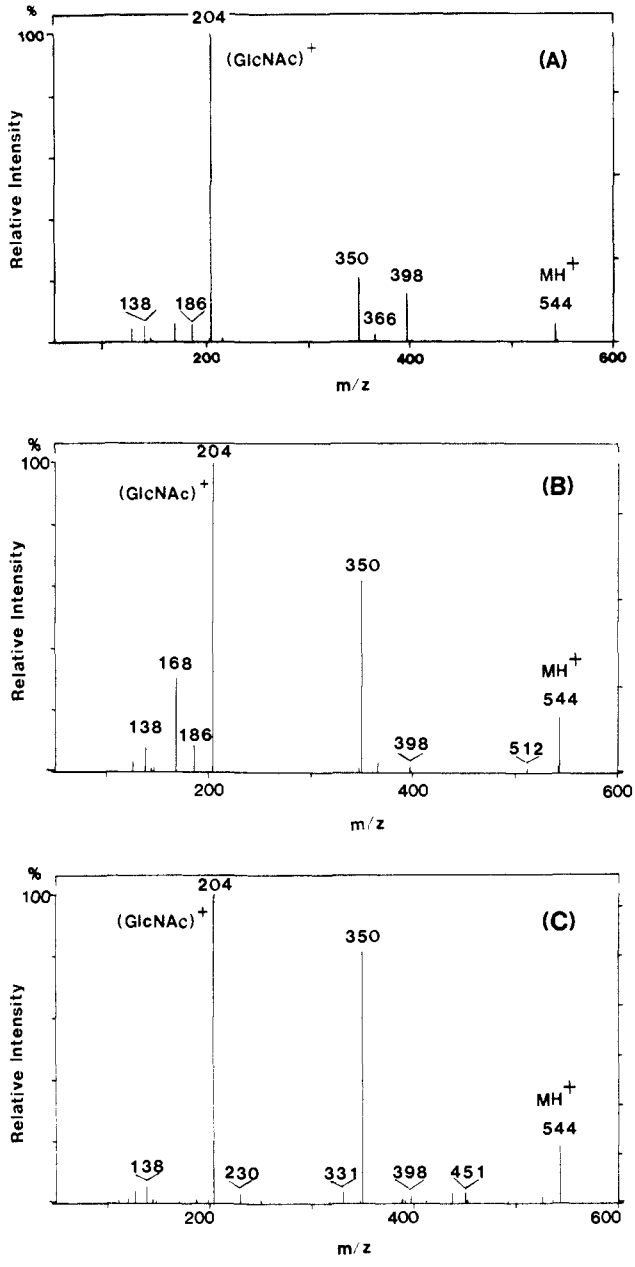

Figure 3. CAD of m/z 544 for F3, F4, and F6. For details, see legend for Figure 2.

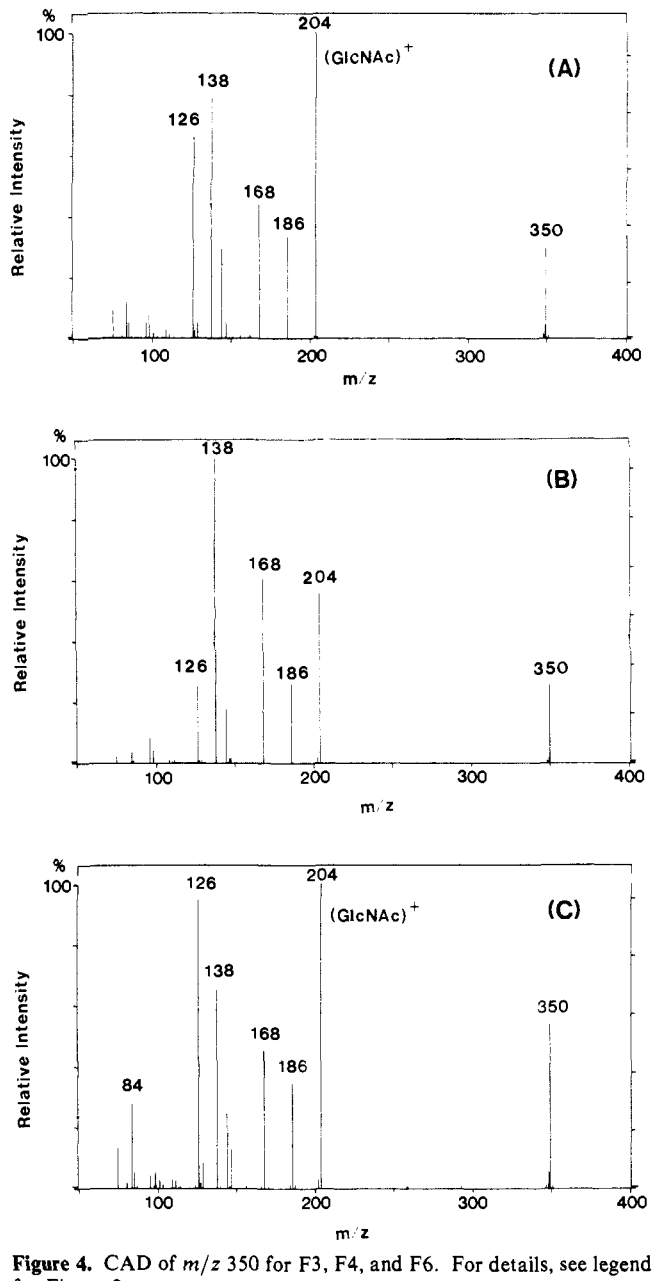

Figure 4. CAD of m/z 350 for F3, F4, and F6. For details, see legend for Figure 2.

each of the three structures, and as with products of 204, any differences represented by formation of m/z 398 are scrambled upon CAD. Thus, the 6-linkage can be distinguished from the 3- and 4-linked fucose by survival of m/z 350. The 3-linkage can be distinguished by the m/z 398:350 ratio in the products of m/z 544. The abundance of m/z 398 indicates that F3 undergoes a more facile cleavage at the fucose–GlcNAc juncture than F4 or F6. Percent survival of m/z 398 is in the order F6 > F4 > F3 in CAD experiments. Additionally, the ion pattern of m/z 204 and its fragments in CAD of m/z 350 is distinct for each linkage position.

Several factors might account for the differences in stability of the various linkages. In F3, the fucose is linked adjacent to the bulky *N*-acetyl group on the 2-position of *N*-acetylglucosamine, and to the secondary hydroxyl on C_4. In F4, fucose is linked adjacent to the secondary hydroxyl on C_3 and to the less bulky C_5 CH_2OH group on GlcNAc, and in F6, the fucose is linked through the hydroxyl attached to the C_6 methylene group yielding extra space between sugar rings. Since the F3 linkage appears to be most crowded and the F6 least, the F3 linkage may be weakened relative to the F4 and F6 linkages. Alternatively, steric forces could cause the fucose–GlcNAc bond in F3 to be most rigid

Table I

	linkage, O_6 position					
	1,3 gg	1,3 gt	1,4 gg	1,4 gt	1,6 gg	1,6
ϕ (H_1–C_1–O_X–C_X)	11.0	6.7	21.4	20.8	43.1	45.
ψ (C_1–O_X–C_X–H_X)	−42.9	−40.3	−49.8	−50.7	−62.0	−57.
(C_1–O_6–C_6–C_5)					177.3	−177.
ω (O_5–C_5–C_6–O_6)	−67.1	62.1	−64.7	64.0	−63.2	63.
steric energy, kcal/mol	29.7	29.5	31.7	31.7	29.4	29

and allow F6 to be most flexible with F4 at an intermediate level. Our hypothesis is that a more flexible molecule would have more possibilities of rotational diffusion to dissipate added vibrational energy from collision events and the transition state representing the reaction coordinate for bond cleavage would be populated less often. Both possibilities were investigated as described below. Another rationale for the more frequent bond rupture in F3 could be more facile loss of substituents near the amide nitrogen, the likely location of charge.

Computer modeling studies were undertaken of the three disaccharide portions of each molecule containing the fucose–>-GlcNAc bond. To assess the steric strain inherent in the different

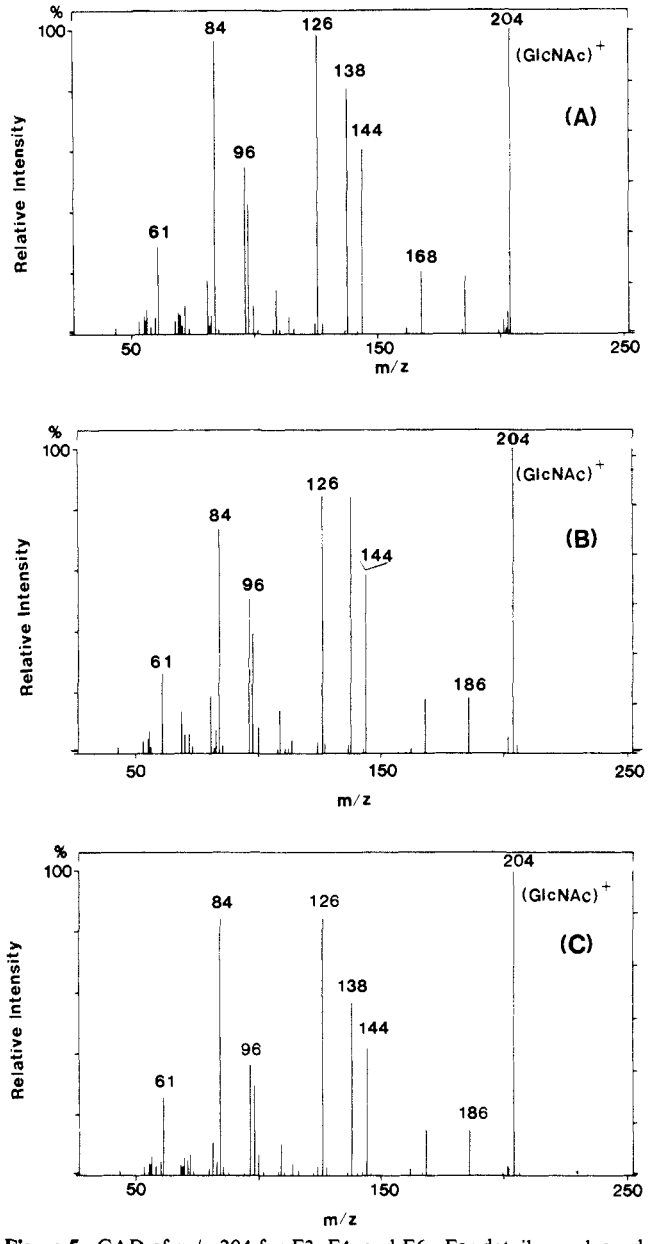

Figure 5. CAD of m/z 204 for F3, F4, and F6. For details, see legend for Figure 2.

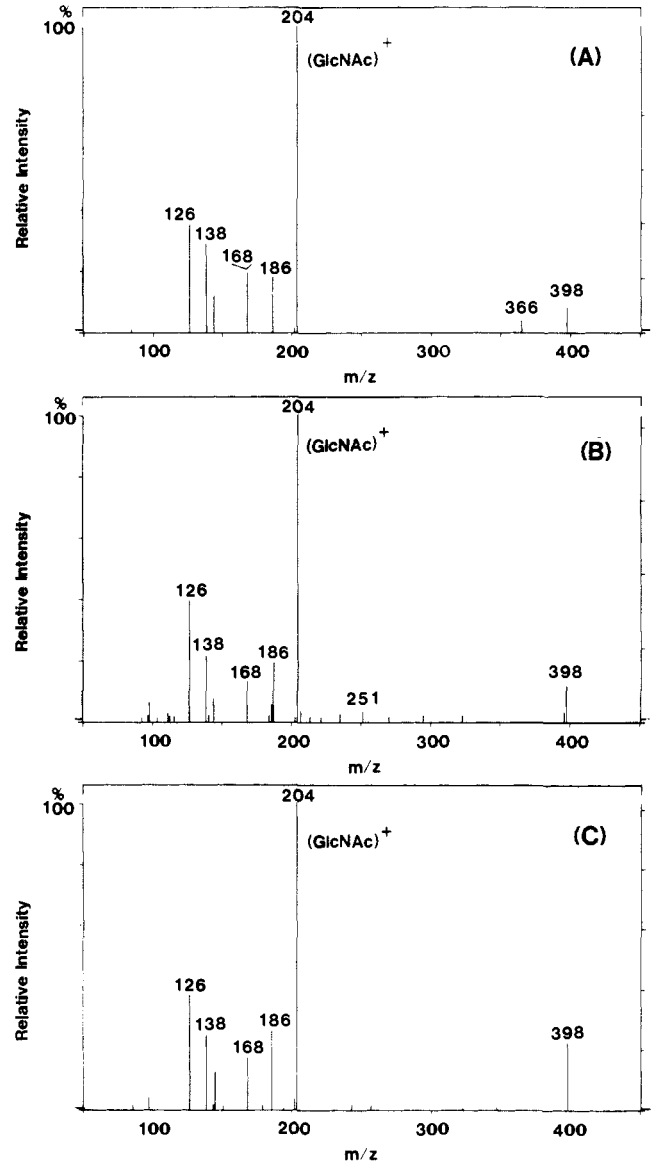

Figure 6. CAD of m/z 398 for F3, F4, and F6. For details, see legend for Figure 2.

linkage patterns, most probable structures were sought and optimized with MMP2 (version 1985). Optimized models of F3, F4, and F6 are shown in Figure 7, and the quantitative results are summarized in Table I.

The differences in steric energy were small enough (±1.2 kcal) to be dependent on the exact choice of force field as well as the linkage. While some attempt was made to position all the hydroxyl hydrogen atoms for lowest energy, slightly lower values might be found. The steric energies are comparable to minima reported for similar disaccharides.[37] In any case, there appears to be no substantial difference in the minimum conformational energies of the various linkages.

To investigate the motional freedom at the three linkages, the above structures and CHEM-X were used to generate simple van der Waals energy surfaces for 360° rotations in 20° increments about the ϕ and ψ bonds. Figure 8 shows both the 2-dimensional contours, with an 11 kcal mol^{-1} cutoff above the minima, and the 3-dimensional inverse sombrero wells cutoff ~55 kcal above the minima. Both types of plot readily indicate that the F3 linkage has the fewest alternate conformations, F4 is intermediate, and F6 is most flexible. The 2-dimensional representations are similar to the more sophisticated results of Homans et al., who investigated the 1→2, 1→3, and 1→6 linkages of α-mannobiose.[38] The 2-dimensional plots indicate that other, major minima were not missed during the steric energy study above and that energies rise quickly outside the areas of the minima.

The 1,3, 1,4, and 1,6 α linkages of glucan dimers were investigated by Gagnaire and Perez.[39] They used similar methods and reported areas of "equiprobable conformations" on the ϕ, ψ surfaces of 8390 (1→3), 4760 (1→4), and 35 800° ^{2} (1→6) at a 6-kcal cutoff. This would be fairly analogous to the present work except for the lack of a GlcNAc group on C_2 in their work and their use of a 6-kcal cutoff instead of a 50-kcal cutoff. Since the stereochemistry of the fucose(1→6)GlcNAc bond in F6 is much less affected by the 2-acetamido group, the ratio of its conformational volume to that of F3, where the C_2 *N*-acetyl is a factor, should be higher than in the work of Gagnaire and Perez. The order of F3 and F4 is reversed, comparing our work with theirs, because the 1,3 linkage for nigerose is distant from the bulky C_6 side group, while in F3 the 1,3 linkage is adjacent to the bulkier

(37) Henrissat, B.; Perez, S.; Tvaroska, I.; Winter, W. T. In *The Structures of Cellulose—Characterization of the Solid States*; Atalla, R. H., Ed.; ACS Symposium Series 340; American Chemical Society: Washington DC, 1987; pp 38–67.

(38) Homans, S. W.; Dwek, R. A.; Rademacher, T. W. *Biochemistry* **1987**, *26*, 6571–6578.

(39) Gagnaire, D.; Perez, S. *Carbohydr. Polym.* **1982**, *2*, 171–191.

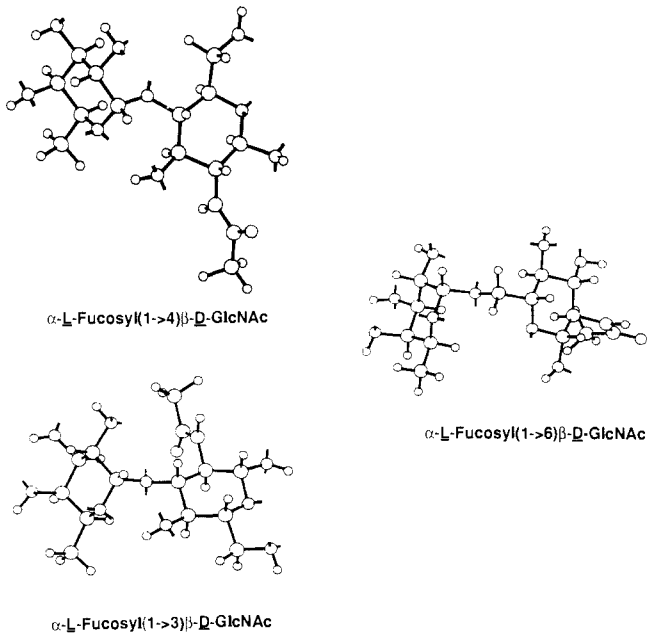

Figure 7. Optimized conformations for the disaccharides F3, F4, and F6. O_6 atoms of the GlcNAc's are in the gt, gt, and gg positions, respectively. All bond lengths, bond angles, and torsion angles were allowed to vary in the MMP2 (version 1985) calculations. These, and similar structures (Table I), served as starting conformations for the rigid residue conformational studies. Large circles with four connected atoms denote carbon atoms, large ones with three connected atoms are nitrogens (hatched) or carbonyl carbons, intermediate circles with two short bonds indicate oxygen atoms with lone pairs of electrons, intermediate circles with one bond are carbonyl oxygens, and the smallest circles are hydrogen atoms. The drawings were made with CHEM-X.

GlcNAc side group. The approximate motional freedoms were quantified by calculating the volumes of the energy wells at various depths above each global minimum. The relative volumes were not very dependent on the depths, so the maximum depth considered, 50 kcal, was used, a figure that is close to the 66 kcal required for scission of an ether link. Setting the volume of the well for F3 to 1.0, the volumes for F4 and F6 were 1.5 and 3.1, respectively. Since the gg and tg versions of F6 also had volumes of ~3.0, F6 has much greater freedom than depicted for only the gt version. (At about the 5-kcal depth, the O_6 group has nearly free rotation.)

While consideration of only van der Waals energies of rigid residues is generally insufficient for rigorously accurate conformational analysis of an oligosaccharide,[40,41] calculations based on van der Waals forces give trends that do not change significantly with additional parameters. A more elaborate study, with flexible residues, takes at least 3 days per disaccharide on a MicroVax 2, and rotation about the ω bond would take 18 times as long using 20° increments. Thus, for comparison in vacuo, and for the purposes of predicting the outcome of collision activation experiments, the calculations were limited to rigid group van der Waals energies because of their speed. Calculations were performed without necessity for consideration of solvation effects because the mass spectral experiments are performed in a vacuum. Before further theoretical development or calculation is warranted, using more detailed parameters, more experimental data are needed.

We assumed that bond scission for the carbon–oxygen bond of the glycosidic linkage would require on the order of 66 kcal added energy and thus chose 55 kcal as a benchmark. As mentioned above, the free energy minima for all three compounds fell to within ±1.2 kcal/mol, not enough to account for the differences observed in CAD spectra. However, upon generating contours at each 5 kcal above the minimum, up to 55 kcal as shown in Figure 8, we noticed that the minimum for F3 was contained in a deep, narrow lake when compared with much more open areas generated for F4 and F6. Since the outlines of the contours (Figure 8A) represented approximately the area of freedom of motion at each level, we computed the volumes of the "lake" below 55 kcal for each of the three compounds. Setting the volume of the lake for F3 at 1.00 (Figure 8B), F4 gave a volume of 1.50 and the gt structure for F6 gave a value of 3.10. Of course, rotating the ω bond for F6 would give other "lakes" of similar volume (3.10). We calculated the gg and tg values, and they also gave near 3.0. An explanation for the interpretation of this data is as follows:

The rate of dissociation of the different positional isomers is best described by transition-state theory for a unimolecular dissociation. Standard RRKM theory assumes a reaction mechanism of the form

$$A + M = A^* + M \qquad A^* = A^+ \qquad A^+ = B$$

and gives the rate as

$$k_r = G(E^+)/G(E^*)/t^+$$

where $G(E^+)$ is the degeneracy of states at the transition state, $G(E^*)$ is the degeneracy of states of the activated complex, and t^+ is the time spent in the transition-state region. $G(E)$ is given (classically) by

$$G(E) = \int d\delta[H(\Upsilon) - E]$$

where Υ stands for the position and momentum of all relevant degrees of freedom that are strongly coupled to the reaction coordinate), H is the hamiltonian, and δ is the delta function. Since the differences between the isomers is at the position of glycosidic oxygen linkage and since the transition state probably corresponds to the two large groups [fucose and GlcNAc(β1→3)Gal-*O*-Me] at large separation where the exact linkage is unimportant, it seems safe to assume that both the density of states at the transition-state energy and the time spent in the transition-state region is the same for all three isomers. Thus, we assume that the differences in dissociation constants is due to differences in the density of states of the molecule in its equilibrium geometry at the dissociation energy. Further, we assume that the reaction coordinate corresponds to a normal mode vibration involving the two large groups (fucose and the GlcNAc-Gal disaccharide) and the oxygen at the linkage. Finally, we expect that only the two rotations of the large groups about the oxygen bonds will be strongly coupled to the reaction coordinate, and hence, we simplify the calculation to three degrees of freedom: the vibration and the two rotations. We realize that the 6-linkage has an additional rotation around the 5,6 carbon–carbon bond which we are considering here to be fixed in one of three most probable orientations. Given these assumptions, it is straightforward to evaluate the density of states. The result is as follows:

$$G(E^*) \propto \int d\psi\, d\phi[E^* - V(\psi,\phi)]\theta[E^* - V(\psi,\phi)]$$

where $\theta(x)$ is the theta function [$\theta(x) = 1$ if $x > 0$ and $= 0$ if $x < 0$) and V is the potential energy surface in the ψ and ϕ coordinates. This quantity is simply the volume of liquid that would fill the potential energy surface (approximated as shown in Figure 7) up to the level E*. The constants of proportionality include the moments of inertia for the rotations and the frequency of the normal mode vibration, which we assume to be the same for all isomers. Thus, our prediction is that k_r should be inversely proportional to $G(E^*)$, with the density of states being given by the above integral.

Thus, comparing the volumes of the lake below 55 kcal gives an approximation of the relative stability of the glycosidic bond to energy imparted to the molecule by collision events. It seems apparent that the 3-linked compound F3 has a far smaller (50% smaller) volume to occupy below 55 kcal of energy (many fewer states) than F4, and only one-third of the volume of a fixed ω (gt) F3. Thus, the relative stability of F6 when compared to F4. The 3-linkage has the least means to distribute this energy among

(40) Melberg, S.; Rasmussen, K. *Carbohydr. Res.* **1979**, *69*, 27–38.
(41) French, A. D. *Biopolymers*, in press.

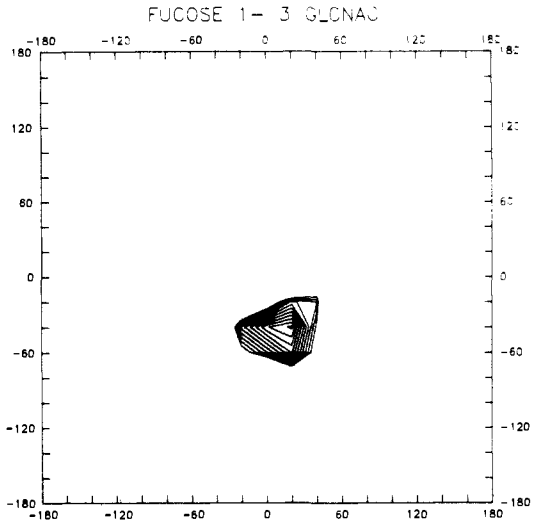

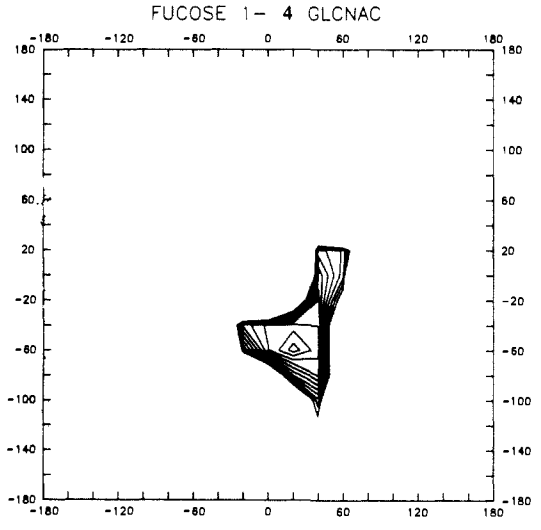

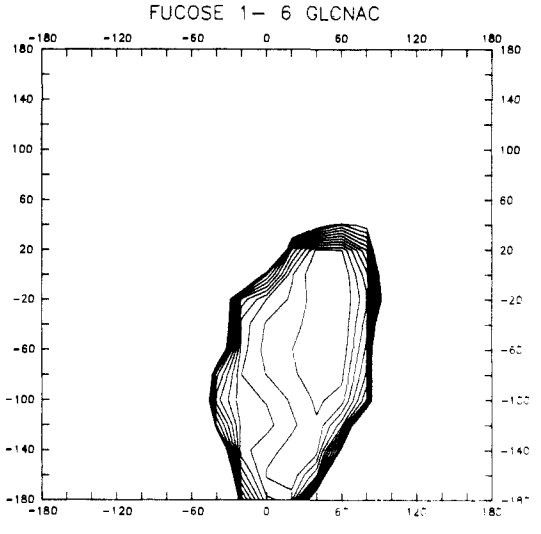

8A

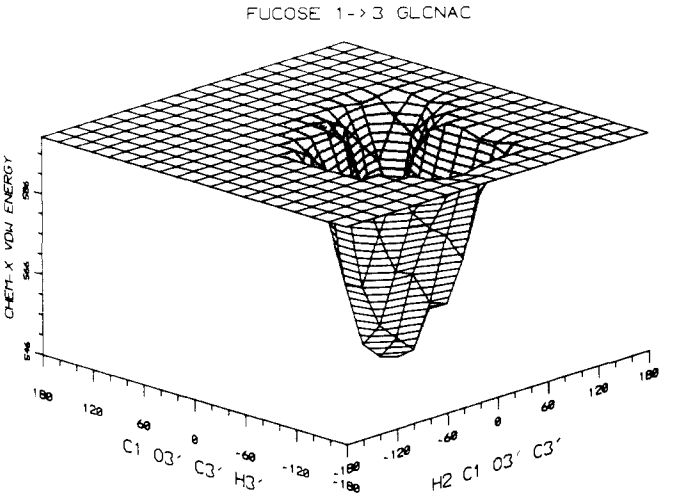

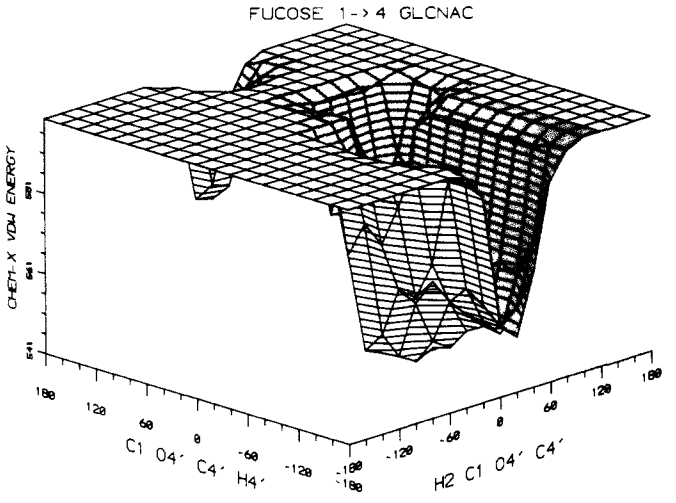

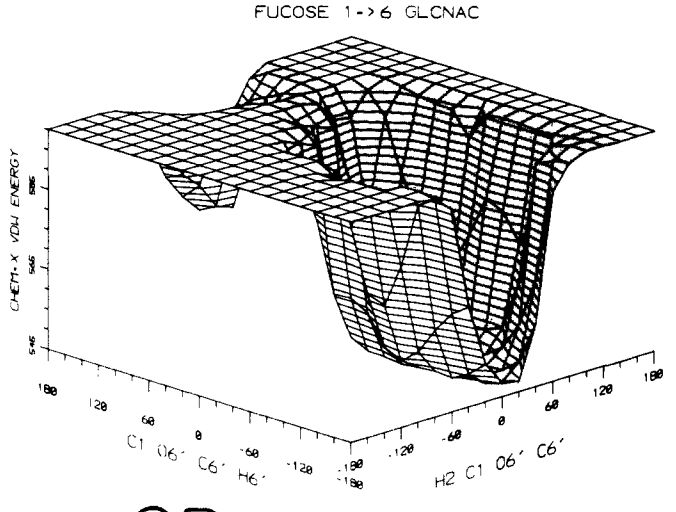

8B

Figure 8. (A) ϕ (horizontal), ψ (vertical) plots of van der Waals energy up to 11 kcal mol^{-1} above the minimum, for F3, F4, and F6. Starting conformations are shown in Table I and Figure 7. The drawings were made with the TOPO program of the SURFER package for IBM-PC compatibles from Golden Software. (B) Energy wells arising from the calculations of van der Waals energy, cut off ~55 kcal above the minima, for F3 (top), F4, and F6 (bottom). The high values of energy are due to the April 1987 CHEM-X algorithm which includes 1,3 interactions that remain constant. The volumes of each well, cut off 55 kcal above the minimum, are 1.0, 1.5, and 3.1 respectively. Shaded areas are the visible, inside surfaces of the wells. The drawings were made with the SURF program of SURFER from Golden Software.

states, resulting in more facile cleavage of this bond. Our conclusion is that CAD spectra of small oligosaccharides may be rich in information on position of linkage and perhaps other stereochemical parameters due to these internal, nonbonding interactions. We are currently studying other series of synthetic saccharides, with differences in position of linkage, anomeric configuration, and with amino and neutral sugars.

Therefore, this is the first systematic MS-CAD-MS and molecular modeling study of a heterooligosaccharide series that clearly shows linkage position in the intact, underivatized compound. FABMS-CAD, in combination with the predictive value for fragmentation using computed motional freedom, shows promise for MS-CAD-MS for precisely fingerprinting oligosaccharide structures based on their internal nonbonding steric energies using calculation of conformational density of states at the transition-state energy corresponding to bond scission.

Registry No. F3, 115921-23-8; F4, 116079-23-3; F6, 116148-08-4.

Adsorption and Decomposition of Dimethyl Methylphosphonate on Platinum(111)

M. A. Henderson and J. M. White*

Contribution from the Department of Chemistry, University of Texas, Austin, Texas 78712.
Received March 16, 1988

Abstract: The interaction of dimethyl methylphosphonate (DMMP) with Pt(111) was studied with high-resolution electron energy loss spectroscopy (HREELS), positive and negative static secondary ion mass spectrometry (SSIMS), temperature-programmed desorption (TPD), and Auger electron spectroscopy (AES). DMMP, a common simulant of more toxic organophosphonate esters, binds strongly and molecularly to Pt(111) at 100 K. HREEL results indicate that it binds through the oxygen lone pairs on the -P=O. Decomposition occurs after heating above 300 K, yielding exclusively CO and H_2 in TPD, with P and a small amount of C left on the surface. The decomposition mechanism first involves PO-CH_3 bond cleavage (300-400 K), with some P-OCH_3 cleavage at high-DMMP coverages, and then P-CH_3 bond cleavage (400-500 K), leaving predominantly PO and an unidentified PO_x species. Both species are stable to at least 500 K. The catalytic applicability of Pt for decomposition of organophosphorus compounds in a nonoxidizing environment is limited by the accumulation of surface P.

1. Introduction

The catalytic decomposition of organophosphorus compounds is of great importance for health and environmental safety.[1] Although these compounds have agricultural, industrial, and military applications, little is known about their molecular chemistry on clean metal and oxide surfaces. Understanding of how organophosphorus compounds interact with these surfaces can lead to better systems for their catalytic decomposition. This paper is a continuation of our work on the interaction of phosphorus-containing molecules with metal and oxide surfaces.[2-9]

Dimethyl methylphosphonate (DMMP), $O{=}P(CH_3)(OCH_3)_2$, is often used to simulate the chemical and structural properties of more toxic organophosphorus compounds.[1] Previous DMMP-substrate research has involved Rh(100),[4] Mo(110),[10] Pt wire,[11] oxidized Fe,[3] Pt/Al_2O_3,[12] Al_2O_3,[13] SiO_2, and Fe_2O_3.[8] These works have been summarized elsewhere,[10] and we focus on those of particular imporance to this study. Graven and co-workers observed catalytic oxidation of DMMP when a DMMP-air or DMMP-N_2 mixture was passed over a commercial alumina-supported Pt catalyst held between 573 and 773 K. The major decomposition products in air were CH_3OH and CO_2, but no CO_2 was observed in the N_2 flow. Catalyst deactivation occurred below reactor temperatures of 720 K; however, a 100% conversion rate was maintained at 770 K. A detailed inelastic electron-tunneling spectroscopy (IETS) study by Templeton and Weinberg[13] has shown that DMMP decomposes on Al_2O_3 in steps according to

$$\text{DMMP} \xrightarrow{295\ \text{K}} \text{MMP} \xrightarrow{573\ \text{K}} \text{MP} \qquad (1)$$

where MMP = methyl methylphosphonate ($CH_3P(OCH_3)O_2$) and MP = methylphosphonate (CH_3PO_3) with CH_3OH emitted at each decomposition step. The P-CH_3 bond was stable to at least 673 K. The durability of the P-CH_3 bond may partially explain the catalytic deactivation observed by Graven et al. below 750 K. However, the role of the Pt in this process has not been determined.

Using laser-induced fluorescence (LIF), Dulcey et al.[11] observed the desorption of PO radicals, along with CH_4, H_2, and CO, when (2.5-7.3) × 10^{-5} Torr DMMP was passed over a Pt wire above

(1) Ekerdt, J. G.; Klabunde, K. J.; Shapley, J. R.; White, J. M.; Yates, J. T., Jr., submitted for publication in *J. Phys. Chem.*
(2) Hedge, R. I.; White, J. M. *J. Phys. Chem.* **1986**, *90*, 2159.
(3) Hegde, R. I.; White, J. M. *Appl. Surf. Sci.* **1987**, *28*, 1.
(4) Hegde, R. I.; Greenlief, C. M.; White, J. M. *J. Phys. Chem.* **1985**, *89*, 2886.
(5) Greenlief, C. M.; Hegde, R. I. White, J. M. *J. Phys. Chem.* **1985**, *89*, 5681.
(6) Mitchell, G. E.; Henderson, M. A.; White, J. M. *J. Phys. Chem.* **1987**, *91*, 3808.
(7) Mitchell, G. E.; Henderson, M. A.; White, J. M.; *Surf. Sci.* **1987**, *191*, 425.
(8) Henderson, M. A.; Jin, T.; White, J. M. *J. Phys. Chem.* **1986**, *90*, 4607.
(9) Hegde, R. I.; Tobin, J.; White, J. M. *J. Vac. Sci. Technol., A* **1985**, *3*, 339.
(10) Smentkowski, V. S.; Hagans, P.; Yates, J. T., Jr., submitted for publication in *J. Phys. Chem.*
(11) Dulcey, C. S.; Lin, M. C.; Hsu, C. C. *Chem. Phys. Lett.* **1985**, *115*, 481.
(12) Graven, W. M.; Weller, S. W.; Peters, D. L. I. & E. C. *Process Des. Dev.* **1966**, *5*, 1983.
(13) Templeton, M. K.; Weinberg, W. H. *J. Am. Chem. Soc.* **1985**, *107*, 97; *Ibid.* **1985**, *107*, 774.

0002-7863/88/1510-6939$01.50/0